JOURNAL OF VIROLOGY, June 2006, p. 5862–5874 Vol. 80, No. 12
0022-538X/06/$08.00+0 doi:10.1128/JVI.02732-05
Copyright © 2006, American Society for Microbiology. All Rights Reserved.

Deregulation of DNA Damage Signal Transduction by Herpesvirus Latency-Associated M2

Xiaozhen Liang,[1] Mary T. Pickering,[2] Nam-Hyuk Cho,[1] Heesoon Chang,[1] Michael R. Volkert,[2] Timothy F. Kowalik,[2] and Jae U. Jung[1]*

Department of Microbiology and Molecular Genetics and Tumor Virology Division, New England Primate Research Center, Harvard Medical School, One Pine Hill Drive, Southborough, Massachusetts 01772,[1] and Department of Molecular Genetics and Microbiology, University of Massachusetts Medical School, Worcester, Massachusetts 01655[2]

Received 29 December 2005/Accepted 27 March 2006

Infected cells recognize viral replication as a DNA damage stress and elicit a DNA damage response that ultimately induces apoptosis as part of host immune surveillance. Here, we demonstrate a novel mechanism where the murine gamma herpesvirus 68 (γHV68) latency-associated, anti-interferon M2 protein inhibits DNA damage-induced apoptosis by interacting with the DDB1/COP9/cullin repair complex and the ATM DNA damage signal transducer. M2 expression constitutively induced DDB1 nuclear localization and ATM kinase activation in the absence of DNA damage. Activated ATM subsequently induced Chk activation and p53 phosphorylation and stabilization without eliciting H2AX phosphorylation and MRN recruitment to foci upon DNA damage. Consequently, M2 expression inhibited DNA repair, rendered cells resistant to DNA damage-induced apoptosis, and induced a G_1 cell cycle arrest. Our results suggest that γHV68 M2 blocks apoptosis-mediated intracellular innate immunity, which might ultimately contribute to its role in latent infection.

DNA damage poses a continuous threat to genomic integrity in mammalian cells. To cope, cells have evolved an elaborate network of sensor, transducer, and effector proteins that coordinate cell cycle progression with the repair of the initiating DNA lesion (4, 31, 34). This decisive signaling network includes ATM (ataxia telangiectasia mutated) and ATR (ataxia telangiectasia and Rad3 related), which transduce the DNA damage signal, and the effector UV-DDB (UV-damaged DNA binding protein complex), which elicits a DNA repair response.

In undamaged cells, ATM resides as a catalytically inactive dimer or higher-order multimer (4, 25). DNA damage triggers auto- or transphosphorylation of the serine residue at position 1981 (Ser1981) in the ATM polypeptide, which leads to the dissociation of inactive ATM complexes into catalytically active ATM monomers (4). Subsequently, ATM signals a checkpoint involving the MRN (Mre11-Rad50-Nbs1) complex (25) and initiates DNA repair by rapidly phosphorylating the histone variant H2AX (6, 15, 52). The phosphorylated H2AX, or γ-H2AX, forms "foci" at double-strand breaks (DSBs) by localizing adjacent to the break as well as at distal genomic loci up to 50 kb away (13, 50, 51). The formation of γ-H2AX foci is believed to promote effective repair by aiding in the accumulation of checkpoint adaptor proteins and the recruitment of DNA repair machinery such as Brca1 and 53BP1 to damage sites (33, 35, 54).

In response to DNA damage, activated ATM signals either a cell cycle arrest or apoptosis by inducing the phosphorylation and activation of the downstream serine/threonine kinases, Chk1, and Chk2 (7, 9, 30, 55). The ATM and Chk kinases subsequently phosphorylate p53 at residues serine 15 and 20 in the N terminus, which results in p53 stabilization. Activated p53 then propagates the signal to arrest or undergo apoptosis depending on cell type and extent of the damage.

In addition to ATM-mediated DNA damage signal transduction, numerous DNA repair systems have been evolved, including nucleotide excision repair (NER), which is a versatile DNA repair pathway that eliminates a wide variety of helix-distorting base lesions. NER operates via two pathways, global genome repair and transcription-coupled repair. Global genome repair repairs DNA damage throughout the entire genome, whereas transcription-coupled repair removes DNA lesions specially from the template strand of actively transcribed genes, resulting in more rapid removal of lesions (18, 43, 47). Impaired NER activity is associated with several rare autosomal recessive disorders in humans, including xeroderma pigmentosum and Cockayne syndrome (44). UV-DDB is a heterodimer complex consisting of either Cockayne syndrome gene A (CSA, p48) or DDB2 (p48) existing in nearly identical complexes via interaction with DDB1 (p127) (17, 57). Both complexes contain the COP9 signalosome (CSN), cullin, SKP1, and Roc1 and display ubiquitin ligase activity differentially regulated by CSN, involved in diverse mechanisms of NER in response to UV (17).

Viral assaults upon the host cell inevitably induce innate antiviral responses designed to prevent completion of the virus life cycle and spread of the infection. Virus replication presents the host cells with large amounts of exogenous genetic material, including DNA ends and unusual structures. Thus, infected cells recognize viral replication as a DNA damage stress and elicit DNA damage signal transduction, which ultimately induces apoptosis as part of host immune surveillance (2, 5, 11, 60). Viruses have evolved a variety of mechanisms to counteract this host innate immune control. In fact, several viruses

* Corresponding author. Mailing address: Tumor Virology Division, New England Primate Research Center, 1 Pine Hill Drive, Southborough, MA 01772. Phone: (508) 624-8083. Fax: (508) 786-1416. E-mail: jae_jung@hms.harvard.edu.

deregulate DNA damage response signaling to facilitate their propagation and persistent infection. For example, paramyxovirus (3, 29, 49) and hepatitis B virus (26) target the DDB complex to avoid host immune attack, and other viruses such as human immunodeficiency virus type 1 (60), herpes simplex virus type 1 (HSV-1) (2, 38, 45), and human cytomegalovirus (37) can activate and exploit a cellular DNA damage response, which aids viral replication. Finally, adenovirus blocks ATM signaling and concatemer formation through targeting the DNA repair complex of MRN for degradation and mislocalization (40).

Herpesviruses persist in their hosts by establishing latent infections and periodically reactivating to produce infectious virus. Gammaherpesviruses (γ-herpesviruses) can establish lifelong latency within lymphocytes and are associated with the development of lymphomas and other cancers (59). Murine γ-herpesvirus 68 (γHV68) is closely related to the primate γ2-herpesviruses, Kaposi's sarcoma-associated herpesvirus, herpesvirus saimiri, and rhesus rhadinovirus (14, 53). Because of the presence of lytic replication, infection by γHV68 in mice can provide a genetically tractable animal model for the study of γ-herpesvirus pathogenesis (42). The analysis of γHV68 gene expression has defined four unique open reading frames, M1, M2, M3, and M4, in the left end of the genome, which do not share homology with other γ-herpesviruses (53). Of particular interest is the M2 protein, which was identified as a latency-associated gene and a target for the host cytotoxic T-lymphocyte response (20). M2 expression has been detected within most latently infected cells (19, 39) and in fibroblast cells upon lytic replication (21). The loss of the M2 gene does not affect the ability of γHV68 to replicate in culture, nor does it affect the acute phase of viral replication in mice following intranasal inoculation (19, 21). However, M2 mutant viruses exhibit a significant decrease in the establishment of latency and reactivation from latency, suggesting that M2 has an important role in viral latent infection (19, 21). Recently, we have shown that M2 effectively induces the downregulation of STAT1 and/or STAT2, resulting in the inhibition of type I and II interferon (IFN)-mediated transcriptional activation, indicating that γHV68 M2 antagonizes the IFN-mediated response that is the major form of host innate immunity (27). Here we report that M2 interacts with and deregulates the cellular DDB1/COP9/cullin-based ubiquitin ligase complex as well as interacting with ATM to escape apoptosis. These results suggest that γHV68 harbors M2 latent protein in order to impede both IFN- and apoptosis-mediated host innate immunities that might ultimately contribute to the establishment and maintenance of latent infection.

MATERIALS AND METHODS

Cell culture, plasmids, and transfection. All cell lines were grown in Dulbecco's modified Eagle's medium (Invitrogen) supplemented with 10% fetal bovine serum and 1% penicillin-streptomycin (Gibco-BRL). Expression vectors encoding M2, glutathione *S*-transferase (GST)–M2 fusion, and their mutants have been previously described (27). Lipofectamine 2000^{H} (Invitrogen) was used for transfection in mouse embryo fibroblasts (MEFs) and NIH 3T3 cells. Calcium phosphate precipitation (Clontech) was used for transfection into 293T cells. Cells stably expressing M2 or its mutants were selected and maintained in the presence of puromycin (2 μg/ml).

Protein purification, GST pull-down assay, and immunoprecipitation. Protein purification and mass spectrometry analysis of M2 binding proteins have been previously described (27). For M2-DDB1 binding assays, cell extracts were prepared and immunoprecipitations were performed as previously described (27).

Cell cycle analysis and immunofluorescence. NIH 3T3 cells stably expressing wild-type (wt) or mutant M2 were treated with 20 μM etoposide (Sigma) for indicated times, trypsinized, and fixed in 70% ethanol for 4 h, followed by staining in propidium iodide (PI) solution (0.1% Triton X-100, 2 mg RNase A, 20 μg/ml PI) at 37°C for 15 min. Immunofluorescent staining was performed as previously described (27). Antibodies used in this study are AU1 (Bethyl Laboratory), Flag (Sigma, St. Louis, Mo.), p53 (Santa Cruz Biotech, Santa Cruz, Calif.), DDB1 (Zymed), γ-H2A (Cell Signaling), or Topro-3 (Molecular Probes, Oregon) for nucleus. Bound antibody was detected using immunoglobulin conjugated to Alexa Fluor 488 or 568 (Molecular Probes) at 1:2,000. Images were obtained using a Leica TCSSP confocal microscope.

RPA. Total RNA was isolated from the cells using TRIzol reagent (Invitrogen). In vitro transcription and RNase protection assays (RPAs) were performed according to the manufacturer's instructions (BD Biosciences). Multiprobe template sets were purchased from BD Biosciences. The housekeeping gene probe L32 and glyceraldehyde-3-phosphate dehydrogenase were included for normalization.

Detection of UV-damaged DNA. Cells grown on four-well chamber slides were UV treated with 2.5 J/m^2 and recovered at the indicated times. Damaged DNA was detected by in situ immunofluorescence staining with specific anti-UV single-stranded DNA (ssDNA) antibody according to the manufacturer's instructions (Trevigen).

Alkaline comet assay. wt MEFs were plated at 1×10^5 cells/well of a six-well plate. The following day, cells were UV treated with 5,000 J/m^2. After 30 min, cells were collected, washed in phosphate-buffered saline, embedded in low-melting-point agarose, aliquoted onto microscope slides, and processed according to the manufacturer's instructions (Trevigen). Briefly, cells were lysed in a high-salt solution for 30 min and then chromosomal DNA was unwound in an alkaline solution for 45 min in the dark. Samples were subjected to electrophoresis and then immersed in alcohol and dried. To visualize the comets, DNA was stained with SYBR green.

Comets were analyzed using the measurement tool in OpenLab software. The lengths of the comet head and tail were recorded for at least 50 comets on two separate slides (total cell number >100) per treatment. The ratio of tail length to head length was calculated, and cells with a ratio of ≥2 were counted positive for DNA breaks. The percentage of cells positive for DNA breaks following UV treatment and the standard deviation for experiments done in triplicate were calculated for each treatment.

RESULTS

The N terminus of M2 interacts with cellular DDB1/COP9/cullin complex, ATM, and histones. To identify proteins interacting with M2, ^{35}S-labeled lysates of murine A20 B lymphocytes were applied to an affinity column of bacterially purified GST-M2. A polypeptide with an apparent molecular mass of 127 kDa specifically interacted with GST-M2 fusion protein, whereas it did not interact with GST alone (Fig. 1A). To further characterize this cellular protein, it was analyzed by mass spectrometry, microsequenced, and matched to known sequences. The 127-kDa band was identified as cellular UV-damaged DNA binding protein 1 (DDB1). Because DDB1 is associated in a heterodimer complex with either DDB2 or CSA (17) and because these DDB complexes exist as part of a large complex with Roc1, COP9, SKP1, and the cullin ubiquitin E3 ligase complex (17, 57), we determined whether M2 interacted with any or all of these proteins by performing immunoprecipitations. As expected, DDB1 interacted with M2 but we also detected M2 interactions with CSN1 and SKP1 (Fig. 1B). Although the cellular DDB complexes may contain cullin 4A, it was not found complexed to M2, which bound cullin 1 (Fig. 1B). Since ATM is a key regulator to signal DNA damage (1) and DDB complexes are associated with cellular chromatin (17), we further tested our hypothesis that M2 might be associated with ATM and chromatin proteins. Indeed, we found

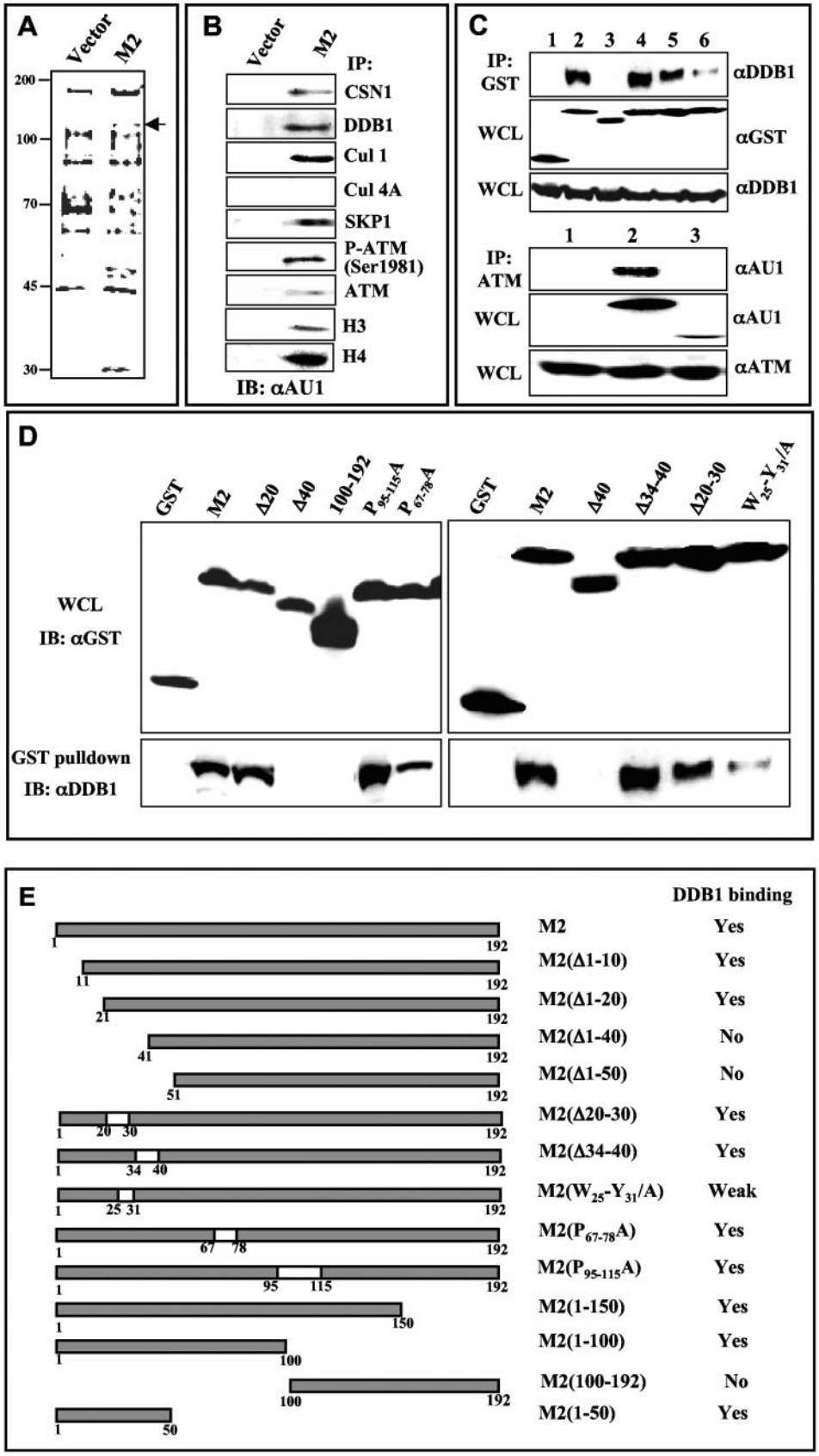
A
Vector
M2
200
100
70
45
30
B
Vector
M2
IP:
CSN1
DDB1
Cul 1
Cul 4A
SKP1
P-ATM (Ser1981)
ATM
H3
H4
IB: αAU1
C
1 2 3 4 5 6
IP: GST
αDDB1
WCL
αGST
WCL
αDDB1
1 2 3
IP: ATM
αAU1
WCL
αAU1
WCL
αATM
D
GST
M2
Δ20
Δ40
100-192
P95-115A
P67-78A
GST
M2
Δ40
Δ34-40
Δ20-30
W25-Y31/A
WCL
IB: αGST
GST pulldown
IB: αDDB1
E
DDB1 binding
M2 Yes
M2(Δ1-10) Yes
M2(Δ1-20) Yes
M2(Δ1-40) No
M2(Δ1-50) No
M2(Δ20-30) Yes
M2(Δ34-40) Yes
M2(W25-Y31/A) Weak
M2(P67-78A) Yes
M2(P95-115A) Yes
M2(1-150) Yes
M2(1-100) Yes
M2(100-192) No
M2(1-50) Yes

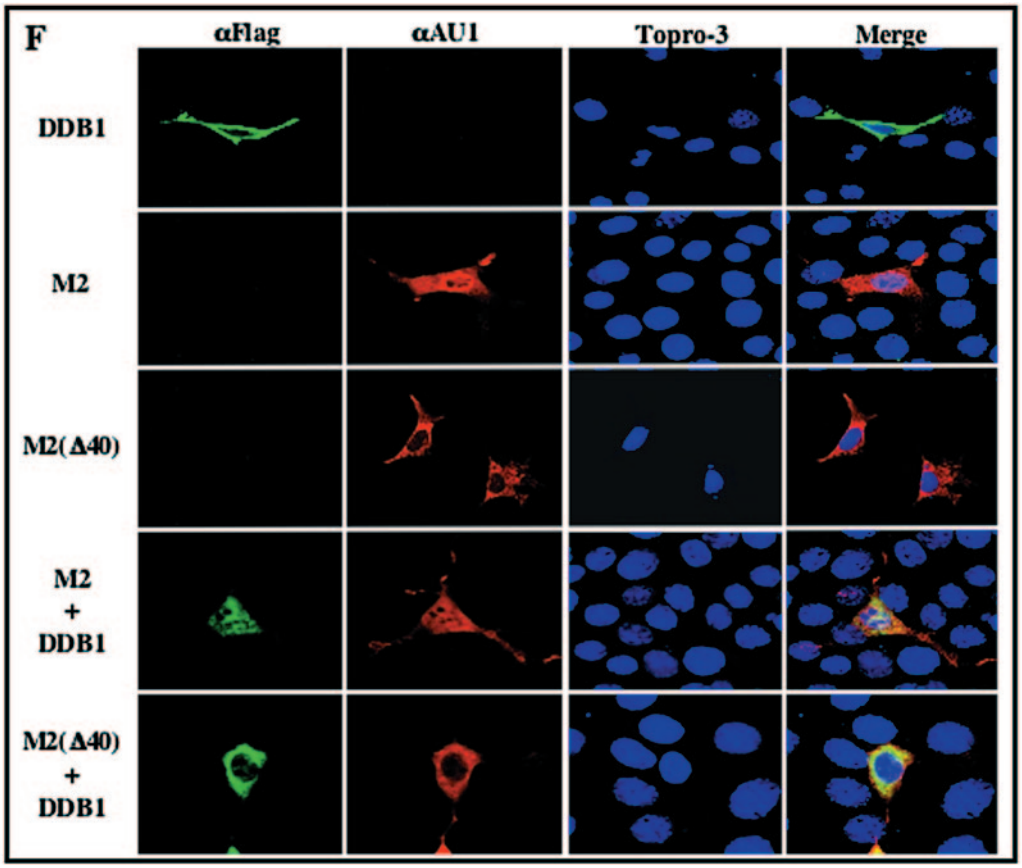

FIG. 1. M2 interacts with the DDB1/COP9/cullin complex, ATM, and histones. (A) Purification of M2-binding cellular proteins. Sodium dodecyl sulfate-polyacrylamide gel electrophoresis analysis of proteins bound to GST-M2 fusion protein or a vector control. The arrow indicates a unique band in the GST-M2 sample, which was identified as DDB1 by mass spectrometry. Numbers at left are molecular masses in kilodaltons. (B) M2 interacts with DDB1/COP9/cullin complex, ATM, and histones. Equal amounts of whole-cell lysates were prepared from 3T3-V- or 3T3-AU1-tagged M2 cells and used for immunoprecipitation with the indicated antibodies, followed by immunoblotting with an anti-AU1 antibody. (C) Identification of DDB1 and ATM-interacting region in M2. (Top panel) NIH 3T3 cells were transiently transfected with GST, GST-M2, or GST-M2 mutant expression construct. At 48 h posttransfection, cell lysates were used for GST pull-down with glutathione-Sepharose beads. Purified proteins were separated by sodium dodecyl sulfate-polyacrylamide gel electrophoresis and analyzed by immunoblotting with an anti-DDB1 antibody. Whole-cell lysates (WCL) were used to detect DDB1 and GST-M2 proteins. Lane 1, GST; lane 2, GST-M2; lane 3, GST-M2(Δ1-40); lane 4, GST-M2(Δ34-40); lane 5, GST-M2(Δ20-30); lane 6, GST-M2(W_{25}-Y_{33}/A). (Bottom panel) 3T3-V, 3T3-M2, and 3T3-M2(Δ1-40) cells were used for immunoprecipitation with an anti-ATM antibody, followed by immunoblotting with an anti-AU1 antibody to detect M2 protein. Whole-cell lysates were used to detect ATM and M2 proteins. Lane 1, 3T3-V; lane 2, 3T3-M2; lane 3, 3T3-M2(Δ1-40). (D) Identification of DDB1 binding region in M2. GST fusions of M2 and its mutants were expressed in NIH 3T3 cells, and their DDB1 binding was examined as described for panel C. (E) Schematic diagram of GST-M2 mutant constructs and summary of DDB1 binding activity of M2. (F) Nuclear localization of DDB1 complex by M2. Shown are confocal images of 3T3 cells transiently transfected with Flag-DDB1, AU1-M2, or AU1-M2(Δ1-40) individually or together. DDB1 protein is stained in green, and M2 proteins are stained in red. Nuclei were stained with Topro-3 (blue).

ATM and the phosphorylated form of ATM (p-ATM), as well as the histone proteins H3 and H4, in the M2 complex (Fig. 1B). The majority of this complex was also detected in the solubilized chromatin fraction (data not shown). These results indicate that M2 protein interacts with the DDB complex and ATM and binds to chromatin-associated proteins.

To further delineate these interactions, cells were transfected with expression vectors containing 14 different GST-M2 mutants and analyzed for interaction with DDB1. We found that most M2 mutants were able to interact with endogenous DDB1 as efficiently as wt M2, except for the M2(Δ1–40) and M2(Δ1–50) mutants (Fig. 1C, D, and E). Additionally, the GST-M2(W_{25}-Y_{33}/A) mutant, which contained alanine substitutions at residues W_{25}, G_{26}, D_{27}, G_{28}, D_{30}, G_{31}, and Y_{33}, showed a significant reduction in the interaction with an endogenous DDB1 (Fig. 1C and D). Interestingly, the interaction of M2 with ATM was similar to the interaction of M2 with DDB1, such that the wt M2, but not M2(Δ1–40), effectively interacted with endogenous ATM (Fig. 1C, bottom panel). These results indicate that the N terminus of M2 is important for interactions with DDB1 and ATM.

DDB1 is predominantly cytoplasmic in an unstressed cell but is rapidly translocated to the nucleus, where it interacts with DDB2 or CSA upon DNA damage (57). When the cellular localization of M2 was examined, we found it primarily in the nucleus of NIH 3T3 cells, with a low level observed in the cytoplasm and at the plasma membrane localization. However, M2(Δ1–40) was localized predominantly in the cytoplasm (Fig.

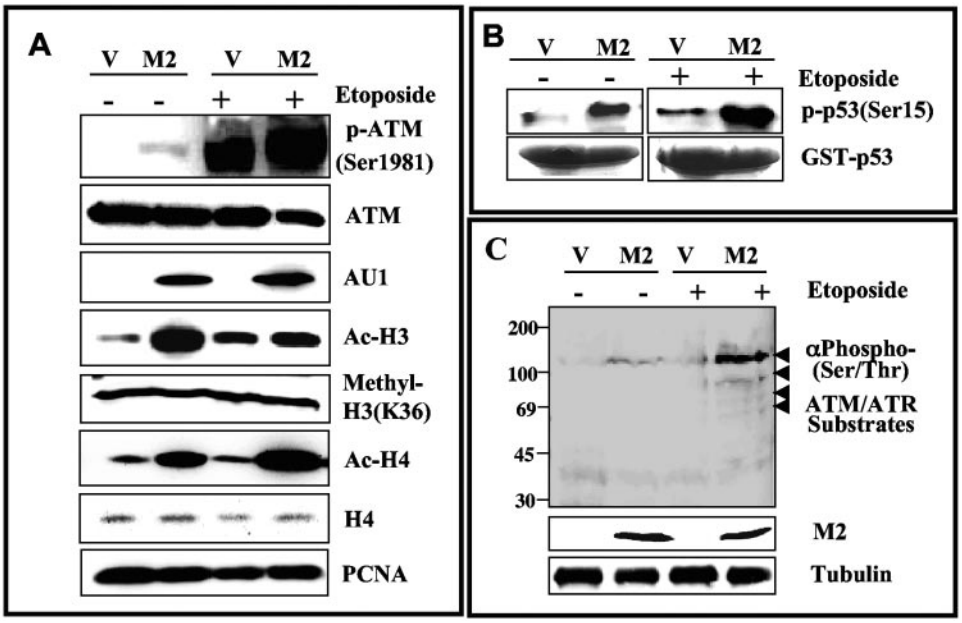

FIG. 2. M2 expression leads to increased ATM activation and histone acetylation. (A) M2 increases levels of activated ATM and acetylated histones. 3T3-V and 3T3-M2 cells were treated with or without 20 μM etoposide for 30 min. Lysates were generated and immunoblotted for ATM, phosphospecific ATM (p-ATM), AU1 (M2), H3 and H4, acetyl-specific histone H3 (Ac-H3) and H4 (Ac-H4), methyl-specific histone H3 (K36), and PCNA. (B) M2 increases ATM kinase activity. Lysates from untreated or etoposide-treated 3T3-V and 3T3-M2 cells were immunoprecipitated with an anti-ATM antibody. The immune complexes were subjected to an in vitro kinase reaction with bacterially purified GST-p53 protein as a substrate followed by immunoblotting with a phosphospecific p53 antibody [p-p53(Ser15)] (top panel). The bottom panel shows the Western blot of the GST-p53 substrate protein. (C) Immunodetection assay of phosphorylated cellular proteins by activated ATM. Equal amounts of polypeptides from 3T3-V and 3T3-M2 cells were immunoblotted with an anti-phospho(Ser/Thr) ATM antibody that specifically reacts with the phosphorylated ATM consensus substrate motif. The middle and bottom panels show M2 and tubulin expression levels, respectively. Arrowheads indicate the phosphorylated cellular proteins that are potential ATM substrates. Numbers at left show molecular masses in kilodaltons.

1F). To test whether the interaction of M2 affects DDB1 localization, NIH 3T3 fibroblast cells were transfected with Flag-tagged DDB1 alone or together with AU1-tagged wt M2 or M2(Δ1-40) mutant. Confocal microscopy showed that DDB1 protein was present principally in the cytoplasm of unstressed cells, whereas it was recruited to the nucleus of NIH 3T3-M2 (3T3-M2) cells (Fig. 1F). In contrast, DDB1 was present in the cytoplasm of cells cotransfected with M2(Δ1-40) (Fig. 1F). These results suggest that M2 may be capable of recruiting DDB1 into the nucleus in the absence of DNA damage stress and that the N-terminal region of M2 is required not only for DDB1 interaction and nuclear recruitment but also for its own nuclear localization.

M2 induces ATM activation and histone acetylation. Because ATM is a key signaling component following DNA damage and we found ATM recruited to the M2/DDB1 complex, we investigated whether M2 affects ATM-mediated DNA damage signal transduction. Levels of phosphorylated, activated ATM (p-ATM) were examined from lysates of untreated or etoposide-treated 3T3-V and 3T3-M2 cells. Etoposide is a topoisomerase II inhibitor that generates DSBs (8) and is known to activate ATM. Undetectable levels of p-ATM were observed in untreated 3T3-V cells, whereas p-ATM was readily detected in untreated 3T3-M2 cells. As expected, etoposide treatment greatly enhanced levels in both cell types (Fig. 2A). To examine whether the p-ATM was active, equal amounts of protein from 3T3-V and 3T3-M2 lysates were immunoprecipitated with an anti-ATM antibody and subjected to an in vitro kinase reaction with bacterially purified GST-p53(AD) as a substrate. We found that ATM kinase activity was significantly higher in 3T3-M2 cells with or without etoposide treatment than in 3T3-V cells (Fig. 2B). Finally, an immunodetection assay using an anti-phospho-(Ser/Thr) ATM antibody that specifically recognizes the p-ATM consensus substrate motif showed that although the phosphorylation of a cellular 120-kDa protein was weakly detected in 3T3-M2 cells before etoposide treatment, phosphorylation levels were markedly increased after etoposide treatment (Fig. 2C). Phosphorylation of 65-, 75-, and 100-kDa proteins was also detected in 3T3-M2 cells but not in 3T3-V cells after etoposide treatment (Fig. 2C). These results indicate that M2 expression significantly increases endogenous ATM kinase activity, which is further enhanced following DNA damage.

Chromatin remodeling has been implicated in inducing ATM phosphorylation and activation (4). In addition, we found that M2 strongly interacted with histones H3 and H4 (Fig. 1B). Thus, we tested whether M2 expression affects the level of acetylation and methylation of histones H3 and H4. Lysates from 3T3-V and 3T3-M2 cells were untreated or treated with etoposide and immunoblotted with anti-acetylated specific histone H3 and H4, anti-methylated specific histone H3 and H4, and anti-histone H3 and H4 antibodies. Acetylation of histone H3 and H4 was markedly increased in 3T3-M2 cells compared to that in 3T3-V cells before and after etoposide treatment (Fig. 2A). Confocal analysis of immunofluorescence also showed enhanced histone H4 acetylation in 3T3-M2

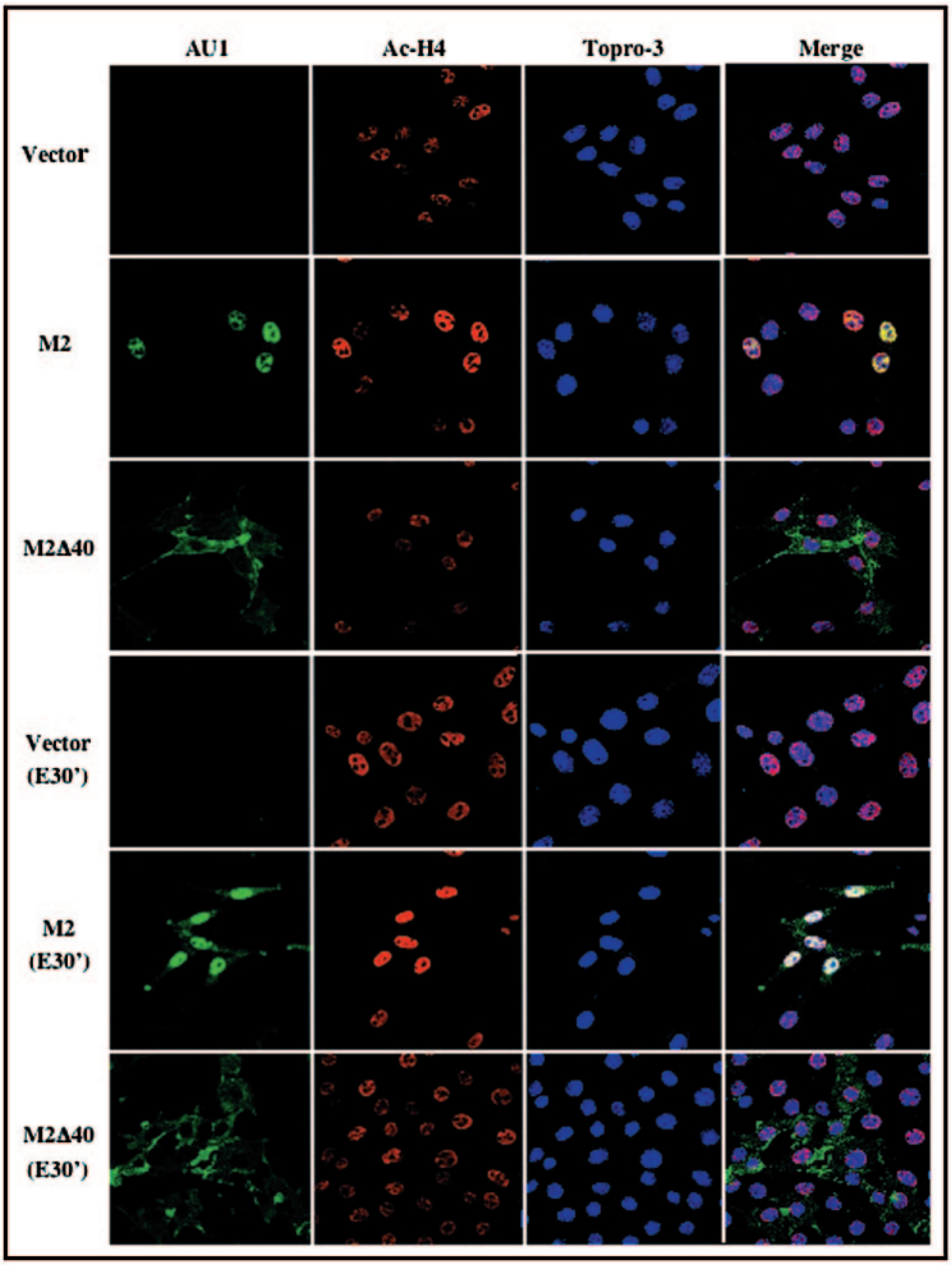

FIG. 3. Increased histone H4 acetylation by M2 expression. Untreated or etoposide-treated 3T3-V, 3T3-M2, and 3T3-M2(Δ1–40) cells were subjected to confocal microscopy with anti-AU1 (green) and anti-acetyl histone H4 antibody (red). Nuclei were stained with Topro-3 (blue).

cells compared to acetylation levels in 3T3-V and 3T3-M2(Δ1–40) cells with or without etoposide treatment (Fig. 3). In contrast, M2 did not appear to affect methylation of histone H3 and H4 regardless of etoposide stimulation (Fig. 2A and data not shown). These results indicate that M2 can increase histone acetylation and that this activity is dependent on the N terminus of M2, which corresponds to the DDB1 and ATM binding region.

Inhibition of γ-H2AX and MRN focus formation by M2. One of the earliest responses to DNA damage is the phosphorylation of the histone variant H2AX by ATM and ATR, which forms γ-H2AX foci (46). Because ATM was significantly activated by M2, we examined the effect of M2 on γ-H2AX focus formation in 3T3-M2, 3T3-M2(Δ1–40), and 3T3-V cells treated with etoposide. γ-H2AX foci were strongly detected in 3T3-V and 3T3-M2(Δ1–40) cells after etoposide treatment (Fig. 4A). By striking contrast, no significant γ-H2AX foci were observed in 3T3-M2 cells regardless of etoposide treatment (Fig. 4A).

γ-H2AX focus formation in the vicinity of the DSBs triggers the accumulation of many components involved in DNA repair. NBS1, a component of the MRN complex, and 53BP1 have been identified as initial sensors of DSBs and are recruited to the γ-H2AX foci, leading to ATM activation (12, 16,

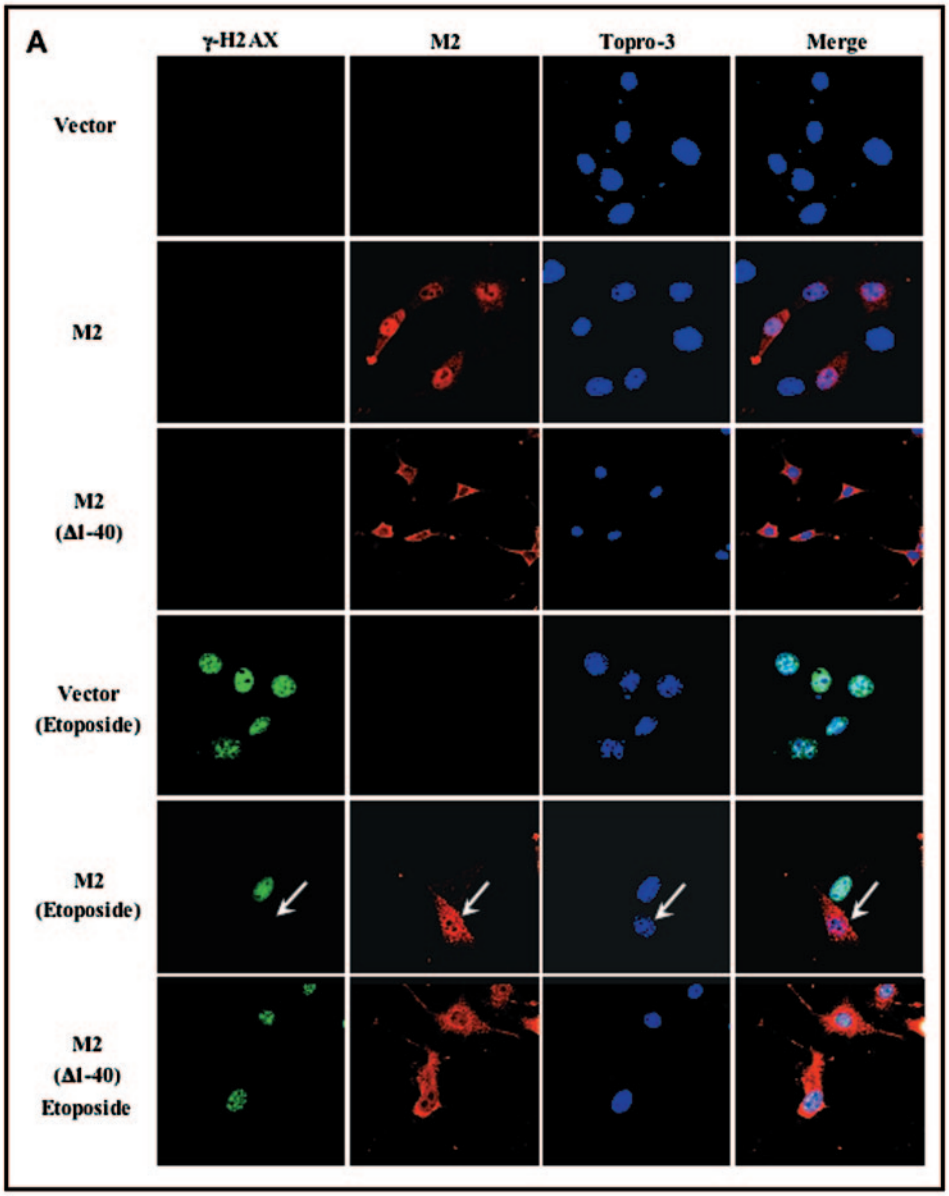

FIG. 4. M2 blocks DNA repair signal transduction. (A) M2 inhibits γ-H2AX focus formation induced by DSB agents. 3T3-V, 3T3-M2, and 3T3-M2(Δ1–40) cells were treated with or without etoposide for 30 min, fixed, permeabilized, and stained with anti-γ-H2AX (green) and anti-M2 (red) antibodies. Nuclei were stained with Topro-3 (blue). Arrows indicate M2-expressing 3T3 cells. (B) M2 inhibits γ-H2AX and MRN focus formation induced by single-strand break agents. 3T3-V, 3T3-M2, and 3T3-M2(Δ1–40) cells were UV irradiated at 10 J/m^2 and left to recover for 40 min. Cells were then fixed, permeabilized, and stained with anti-γ-H2AX (green) and anti-phosphospecific NBS1 (red) antibodies. Nuclei were stained with Topro-3 (blue). (C) M2 suppresses 53BP1 recruitment. 3T3-V, 3T3-M2, and 3T3-M2(Δ1–40) cells were UV irradiated at 10 J/m^2 and left to recover for 40 min. Cells were then fixed, permeabilized, and reacted with anti-γ-H2AX (green) and anti-53BP1 (red) antibodies. Nuclei were stained with Topro-3 (blue).

22, 25, 36, 58). To assess whether M2 expression also prevents the recruitment of DNA damage repair proteins, we determined whether phosphorylated NBS1 (p-NBS1) and 53BP1 were also recruited to foci following DNA damage. We found γ-H2AX foci in 3T3-V and 3T3-M2(Δ1–40) cells immediately after UV irradiation, and the intensity and number of the foci markedly increased concomitantly with the localization of 53BP1 and MRN foci, as detected by p-NBS (Fig. 4B and 4C). Additionally, γ-H2AX foci localized adjacent to p-NBS foci in these cells (Fig. 4B). In striking contrast, 3T3-M2 cells showed neither γ-H2AX nor p-NBS focus formation following UV exposure (Fig. 4B). These results demonstrate that despite ATM kinase activation, M2 expression blocks the ability of ATM to induce γ-H2AX and 53BP1 focus formation and p-NBS recruitment and that the ATM and DDB1 binding region of M2 is required.

M2 inhibits DNA repair signal transduction. Because of the surprising finding that M2-mediated ATM activation did not

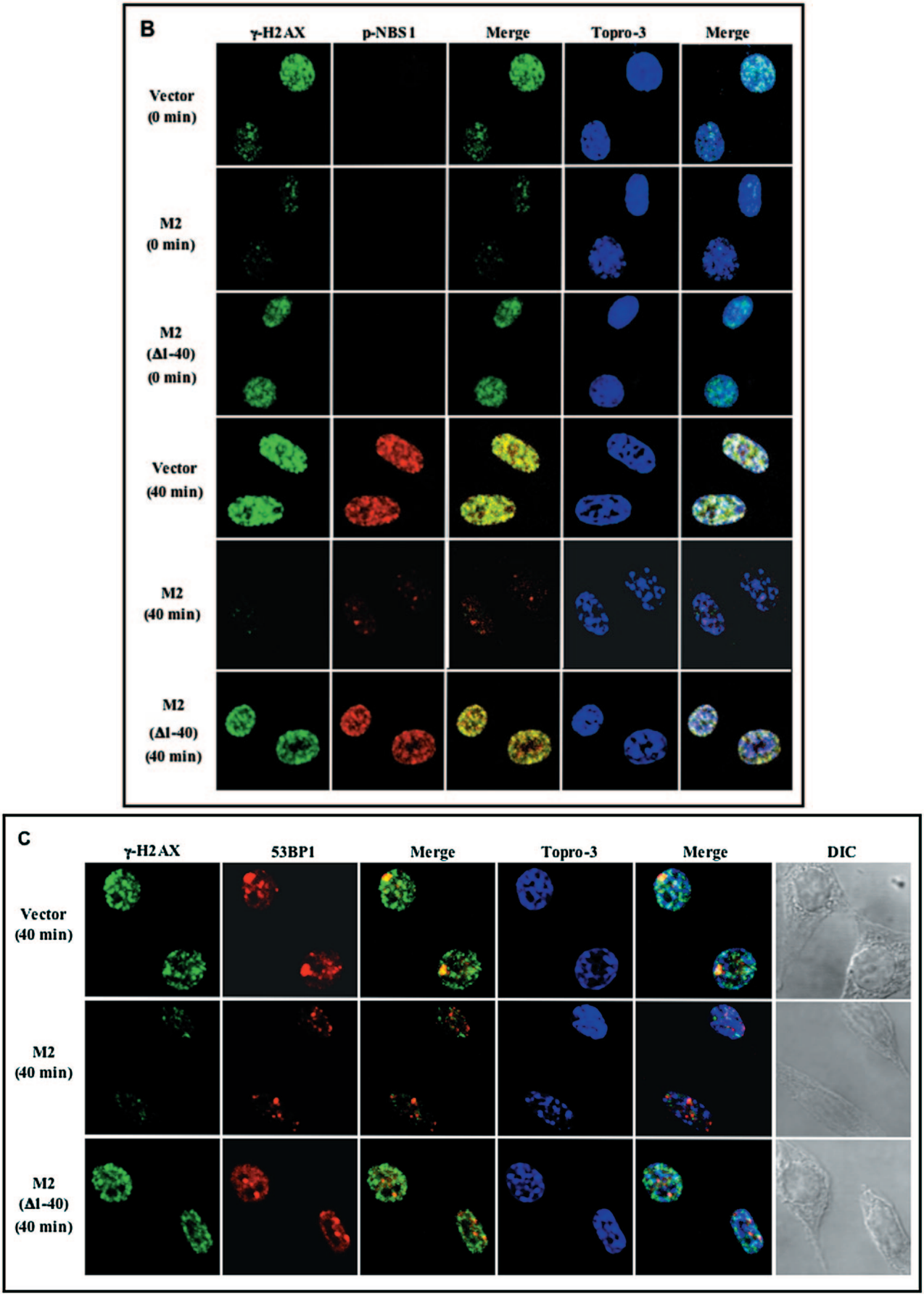

FIG. 4—*Continued.*

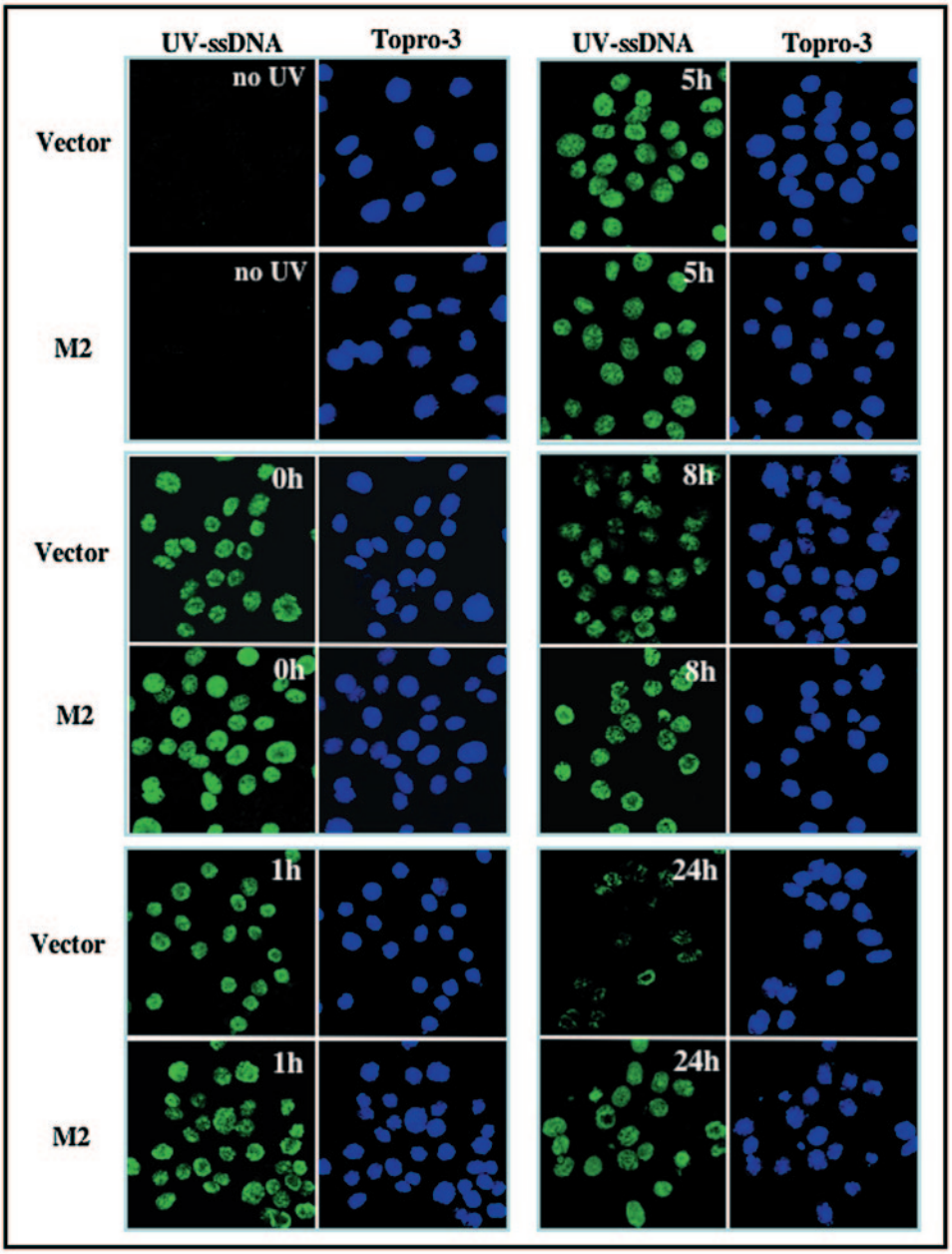

FIG. 5. In situ fluorescent immunohistochemistry to detect DNA damage induced by UV irradiation. 3T3-V and 3T3-M2 cells were UV irradiated at 2.5 J/m^2 and left to recover for the indicated times. Cells were then fixed, permeabilized, and reacted with an anti-UV ssDNA antibody (green). Nuclei were stained with Topro-3 (blue).

lead to γ-H2AX and MRN focus formation, we tested whether M2 expression affected the levels of DNA damage and/or repair. In situ fluorescent immunohistochemistry was performed to detect the damaged DNA using an anti-UV ssDNA antibody that specifically recognizes dipyrimidine photoproducts in single-stranded DNA upon exposure to UV light (41). 3T3-V and 3T3-M2 cells were treated with UV, fixed at various times following damage, and stained with an anti-UV ssDNA antibody. Immediately following UV exposure, 3T3-V and 3T3-M2 cells showed similar levels of DNA damage based on the intensity of anti-UV ssDNA antibody reactivity (Fig. 5). No detectable difference in the number and size of the damaged DNA foci was detected until 5 h post-UV exposure (Fig. 5), indicating that M2 expression did not affect the initial level of DNA damage. However, the number and intensity of damaged DNA foci started to decline in 3T3-V cells at 8 h post-UV exposure and were dramatically reduced at 24 h post-UV exposure, whereas the foci remained high in the 3T3-M2 cells throughout the recovery period (Fig. 5). These results indicate that DNA repair is significantly impaired in 3T3-M2 cells, whereas foci decrease in 3T3-V cells over time.

To gain insight into the inhibition of DNA repair observed

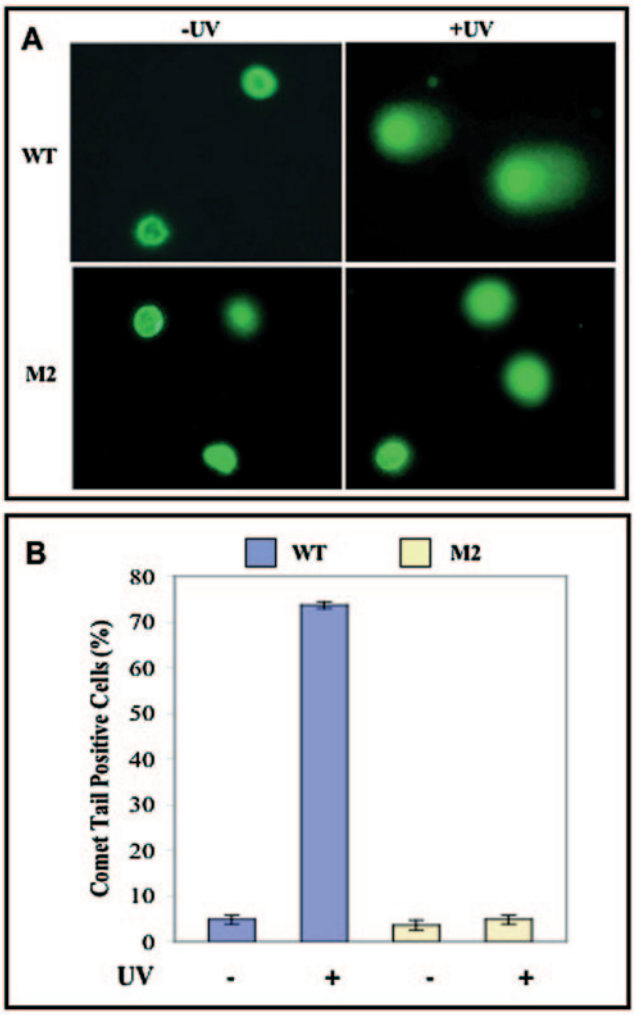

FIG. 6. M2 inhibits DNA repair signal transduction. (A) Comet tail formation. MEF-V and MEF-M2 cells were subjected to alkaline comet assays 30 min after treatment with or without 5,000 J/m^2 UV. DNA from individual cells was visualized by staining with SYBR green. (B) Quantitation of alkaline comet assay. Cells were treated as in panel A, and the head and tail lengths were measured for at least 100 cells per treatment. The percentages of positive cells and the standard deviations are reported for an experiment done in triplicate.

in M2-expressing cells, we performed the comet assay, also termed single cell gel electrophoresis, which is a highly sensitive fluorescent microscopic method to examine DNA damage and repair in individual cells. Stable clones of M2 or vector control-transfected primary MEFs (MEF-M2 or MEF-V) were treated with a high dose of UV and subjected to the comet assay. We found that over 78% of MEF-V cells were comet tail positive, whereas less than 5% of MEF-M2 cells were comet tail positive under the same conditions (Fig. 6A and B). Because the major species of DNA breaks in response to UV is dipyrimidine photoproducts, in order for cells to manifest as comet tail positive, DNA repair mechanisms must be intact. Our results collectively suggest that M2 expression likely blocks DNA damage-sensing activity and thereby inhibits cellular damaged DNA repair activity.

M2 inhibits DNA damage-induced apoptosis. Upon genotoxic stress, activated ATM initiates the repair signaling cascade leading to the resolution of DSBs as well as signaling cell cycle arrest or apoptosis (32). Because M2-induced ATM activation did not activate the DNA repair pathway, we tested whether it affects cell cycle control or apoptosis. 3T3-V and 3T3-M2 cells were treated with etoposide for the indicated times, and their lysates were used for immunoblotting with a panel of phosphospecific antibodies to analyze activation of proteins involved in arrest and apoptosis. We observed elevated levels of total p53 as well as increased levels of phospho-p53 at Ser15 and Ser20 in response to etoposide treatment of 3T3-M2 cells. Interestingly, phospho-p53 at Ser6 levels, which is potentially induced by casein kinase I, decreased after etoposide treatment in 3T3-M2 cells (Fig. 7A). Similarly, phospho-Chk1 levels increased and phospho-CDC2 levels decreased in 3T3-M2 cells compared to 3T3-V cells (Fig. 7A).

When we looked at the effect of M2 on MDM2, p21, and CDC2, we found that MDM2 and p21 levels were considerably higher in 3T3-M2 cells than in 3T3-V cells (Fig. 7B). In contrast, total CDC2 levels were downregulated in etoposide-treated 3T3-M2 cells, similar to the observed decrease in phospho-CDC2 (Fig. 7A and B). Next, RPAs were performed to determine the transcript levels of p53 and other cell cycle regulatory genes including CDK1, MDM2, cyclin D1, and p21. M2 expression did not significantly affect mRNA levels of p53, CDK1, MDM2, and cyclin D1 regardless of etoposide treatment (Fig. 7C). In addition, despite a robust increase of p21 protein level, only a slight increase of p21 transcript was detected in etoposide-treated 3T3-M2 cells compared to 3T3-V cells throughout etoposide treatment (Fig. 7C). These results suggest that although M2-induced ATM kinase signaling did not lead to the activation of a DNA repair pathway, it markedly activated proteins involved in cell cycle arrest.

Finally, we tested the effect of M2-induced ATM activation on the cell cycle profile and apoptosis. 3T3-V, 3T3-M2, and 3T3-M2(Δ1–40) cells were treated with etoposide, stained with propidium iodide, and analyzed by fluorescence-activated cell sorting to measure their cell cycle profile and apoptosis. High levels (41%) of 3T3-V cells treated with etoposide had <2N DNA content and were considered to be apoptotic, whereas apoptosis levels were slightly reduced but still significant (28%) in 3T3-M2(Δ1–40) cells. In contrast, less than 6% of 3T3-M2 cells were apoptotic following etoposide treatment, with the majority of cells arrested in G_1 (Fig. 7D). These results indicate that M2 expression renders cells resistant to DNA damage-induced apoptosis and M2-induced ATM activation ultimately leads to a G_1 cell cycle arrest.

DISCUSSION

Upon viral infection, the major defense mounted by the host innate immune system is activation of the IFN- and apoptosis-mediated antiviral pathway. In order to complete their life cycle, viruses that are obligatory intracellular parasites must modulate these host immune responses. We have previously shown that the γHV68 latency-associated M2 protein effectively downregulates STAT1 and STAT2, resulting in the inhibition of type I and II IFN-mediated transcriptional activation. Here, we demonstrate that M2 interacts with ATM, a

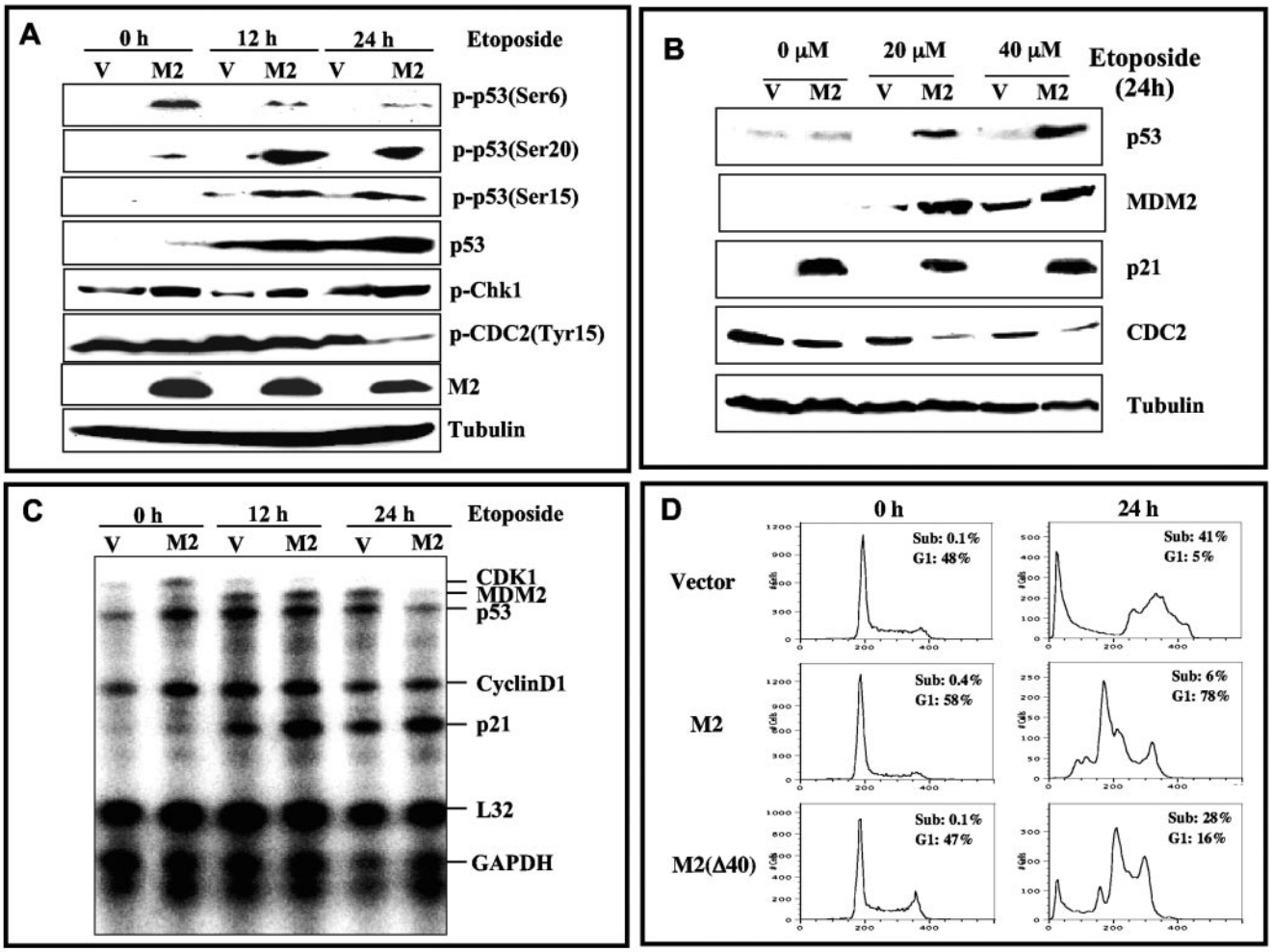

FIG. 7. M2 inhibits etoposide-induced apoptosis. (A) Phosphorylation of cellular cell cycle regulatory proteins. 3T3-V and 3T3-M2 cells were treated with 20 μM etoposide for the indicated times. Whole-cell lysates were reacted with various antibodies as indicated at the right side of the figure. (B) M2 increases cellular cell cycle regulatory protein levels. 3T3-V and 3T3-M2 cells were treated with etoposide for the indicated time. Whole-cell lysates were then reacted with various antibodies as indicated at the right side of the figure. (C) RNase protection assay. 3T3-V and 3T3-M2 cells were treated with etoposide for the indicated times, and their total RNA was isolated by phenol-chloroform extraction, DNase I treated, and then subjected to RPA using the RPA kit (BD Pharmingen). GAPDH, glyceraldehyde-3-phosphate dehydrogenase. (D) Cell cycle analysis. 3T3-V, 3T3-M2 (M2), and 3T3-M2(Δ1–40) cells were treated with or without 20 μM etoposide for 24 h. Cells were then stained for chromosomal DNA with PI and analyzed by flow cytometry. Numbers indicate the percentages of cells with less than 2N DNA content, representing apoptotic cells (Sub) and the percentages of cells in the G_1 cell cycle phase (G1). Results presented are representative of three individual experiments.

DNA damage signal transducer, and the DDB1/COP9/cullin DNA damage effector complex. This interaction blocked DNA damage-sensing activity as well as DNA damage repair activity, thereby rendering cells resistant to DNA damage-induced apoptosis. These results indicate that γHV68 encodes M2, a latency-associated gene, to antagonize both IFN- and apoptosis-mediated host innate immunities and thus is important in establishing and maintaining viral latency in infected animals.

Simian virus 5 (SV5)- and human parainfluenza virus 2 (hPIV2)-encoded V proteins induce polyubiquitination and degradation of STAT1 and STAT2 by interacting with the DDB1/COP9/cullin ubiquitin ligase complex (48, 49). Similarly, hepatitis B virus X protein also interacts with the DDB1/COP9/cullin complex, leading to interference with cell growth and viability despite a lack of homology with SV5 and hPIV2 V protein. γHV68 M2 lacks homology with SV5 and hPIV2 V protein and yet interacts with the DDB1/COP9/cullin complex, resulting in the ubiquitination of STAT1/2 (unpublished data) and deregulation of DNA damage/repair signaling. Thus, while these viral proteins do not share any recognizable sequences or motifs, these viruses have evolved mechanisms to target the cellular DDB1/COP9/cullin complex, which achieves diverse effects on cellular physiology. Besides targeting of the DDB1/COP9/cullin complex, M2 expression also leads to ATM activation. Mutational studies indicated that the N terminus of M2 was essential for binding to both the DDB1/COP9/cullin complex and ATM kinase. However, it is not clear from the architecture of the M2 complex whether ATM was recruited into the M2/DDB1/COP9/cullin complex through a direct interaction with M2 or through a component of the DDB1/COP9/

cullin complex. Regardless of a direct or indirect interaction, the M2/DDB1/COP9/cullin complex preferentially contained the activated p-ATM. Our results suggest that M2 functions as a physical or functional adaptor linking the DNA damage-sensing pathway and the DNA repair pathway, ultimately uncoupling both pathways from the DNA damage response.

Cellular chromatin remodeling has been implicated in inducing ATM phosphorylation and activation (4). We showed that M2 not only interacted with histones H3 and H4 but also constitutively enhanced their acetylation in the absence of ectopic genotoxic stress, indicating that M2 may cause chromatin remodeling and lead to ATM activation. However, M2-induced activation of ATM did not lead to increased DNA damage signaling, as observed from impaired γ-H2AX and 53BP1 focus formation and lack of MRN recruitment in response to DNA damage. Thus, enhanced acetylation of H3 and H4 by M2 expression leads to ATM activation but downstream signaling in response to ATM activation is impaired, resulting in defective DNA damage sensing and DNA repair.

Recent reports have shown that viruses evolve a variety of mechanisms to manipulate DNA damage signaling for their replication and propagation (24, 28, 56). As part of the host response to adenovirus replication, MRN plays a role in the generation of concatemers of the double-stranded viral genome, which is too large to be packaged into virions (40). To counteract this host response, adenovirus encodes E4, which induces the reorganization and degradation of the MRN complex, leading to deregulated genomic stability and contributing to potential viral "hit-and-run" transformation (40). While adenovirus dismantles the host machinery to evade processing of the viral genome, HSV-1 and human cytomegalovirus activate and exploit the cellular DNA damage response to aid their viral replication (28, 37, 38, 45). When this cellular response is abrogated in nonneuronal cells, however, formation of HSV-1 replication centers is retarded, and viral production is compromised. In contrast, HSV-1 replication centers fail to mature in neurons, and the DNA damage response is not initiated, suggesting that the failure of neurons to mount a DNA damage response to HSV-1 may contribute to the establishment of latency (28). Our results raise the possibility that γHV68 M2 prevents initiation of an ATM-mediated DNA damage response that may function in the establishment of latency and reactivation from latency. A more detailed study is necessary to address this question.

Upon viral infection, the major defense mounted by the host immune system is activation of the IFN-mediated antiviral pathway. Furthermore, infected cells also recognize virus replication as DNA damage stress and elicit a DNA damage response, which ultimately induces apoptosis as part of host immune surveillance (2, 5, 10, 11, 24, 37, 60). In order to complete their life cycle, viruses must modulate host IFN- and apoptosis-mediated immune surveillance. Inhibition of IFN- and apoptosis-mediated innate immunity during latency is important for viral persistence in the face of immune attack, whereas inhibition of IFN- and apoptosis-mediated innate immunity during lytic replication also allows viruses to complete lytic replication for subsequent dissemination (23). The latency-associated M2 protein is necessary for the establishment of latency and reactivation from latency (19–21, 39). Thus, M2-mediated inhibition of IFN and apoptosis signaling likely protects cells with latent γHV68 infection or cells undergoing reactivation from host innate immunity, which is essential for chronic lifelong infection. In summary, we demonstrate a novel immune evasion mechanism of γHV68 where latency-associated M2 targets the cellular DDB1/COP9/cullin DNA repair complex and ATM signal transducer. However, instead of activating a downstream DNA damage and repair response, M2 uses these complexes to abrogate IFN- and apoptosis-mediated innate immunity, contributing to viral latency.

ACKNOWLEDGMENTS

We thank S. Gygi for mass spectrometry analysis, K. Boisvert for confocal microscopy, and members of our laboratory for helpful discussion and comments.

This work was partly supported by U.S. Public Health Service grants CA31363, CA082057, CA91819, CA86038, and RR00168. X. Liang is a Leukemia & Lymphoma Fellow.

REFERENCES

1. **Abraham, R. T., and R. S. Tibbetts.** 2005. Cell biology. Guiding ATM to broken DNA. Science **308:**510–511.
2. **Aita, K., H. Irie, A. H. Koyama, A. Fukuda, T. Yoshida, and J. Shiga.** 2001. Acute adrenal infection by HSV-1: role of apoptosis in viral replication. Arch. Virol. **146:**2009–2020.
3. **Andrejeva, J., E. Poole, D. F. Young, S. Goodbourn, and R. E. Randall.** 2002. The p127 subunit (DDB1) of the UV-DNA damage repair binding protein is essential for the targeted degradation of STAT1 by the V protein of the paramyxovirus simian virus 5. J. Virol. **76:**11379–11386.
4. **Bakkenist, C. J., and M. B. Kastan.** 2003. DNA damage activates ATM through intermolecular autophosphorylation and dimer dissociation. Nature **421:**499–506.
5. **Boyer, J., K. Rohleder, and G. Ketner.** 1999. Adenovirus E4 34k and E4 11k inhibit double strand break repair and are physically associated with the cellular DNA-dependent protein kinase. Virology **263:**307–312.
6. **Burma, S., B. P. Chen, M. Murphy, A. Kurimasa, and D. J. Chen.** 2001. ATM phosphorylates histone H2AX in response to DNA double-strand breaks. J. Biol. Chem. **276:**42462–42467.
7. **Buscemi, G., P. Perego, N. Carenini, M. Nakanishi, L. Chessa, J. Chen, K. Khanna, and D. Delia.** 2004. Activation of ATM and Chk2 kinases in relation to the amount of DNA strand breaks. Oncogene **23:**7691–7700.
8. **Caldecott, K., G. Banks, and P. Jeggo.** 1990. DNA double-strand break repair pathways and cellular tolerance to inhibitors of topoisomerase II. Cancer Res. **50:**5778–5783.
9. **Caspari, T.** 2000. How to activate p53. Curr. Biol. **10:**R315–R317.
10. **Castillo, J. P., F. M. Frame, H. A. Rogoff, M. T. Pickering, A. D. Yurochko, and T. F. Kowalik.** 2005. Human cytomegalovirus IE1-72 activates ataxia telangiectasia mutated kinase and a p53/p21-mediated growth arrest response. J. Virol. **79:**11467–11475.
11. **Cuconati, A., C. Mukherjee, D. Perez, and E. White.** 2003. DNA damage response and MCL-1 destruction initiate apoptosis in adenovirus-infected cells. Genes Dev. **17:**2922–2932.
12. **Difilippantonio, S., A. Celeste, O. Fernandez-Capetillo, H. T. Chen, B. Reina San Martin, F. Van Laethem, Y. P. Yang, G. V. Petukhova, M. Eckhaus, L. Feigenbaum, K. Manova, M. Kruhlak, R. D. Camerini-Otero, S. Sharan, M. Nussenzweig, and A. Nussenzweig.** 2005. Role of Nbs1 in the activation of the Atm kinase revealed in humanized mouse models. Nat. Cell Biol. **7:**675–685.
13. **Downs, J. A., S. Allard, O. Jobin-Robitaille, A. Javaheri, A. Auger, N. Bouchard, S. J. Kron, S. P. Jackson, and J. Cote.** 2004. Binding of chromatin-modifying activities to phosphorylated histone H2A at DNA damage sites. Mol. Cell **16:**979–990.
14. **Efstathiou, S., Y. M. Ho, S. Hall, C. J. Styles, S. D. Scott, and U. A. Gompels.** 1990. Murine herpesvirus 68 is genetically related to the gammaherpesviruses Epstein-Barr virus and herpesvirus saimiri. J. Gen. Virol. **71:**1365–1372.
15. **Friesner, J. D., B. Liu, K. Culligan, and A. B. Britt.** 2005. Ionizing radiation-dependent gamma-H2AX focus formation requires ataxia telangiectasia mutated and ataxia telangiectasia mutated and Rad3-related. Mol. Biol. Cell **16:**2566–2576.
16. **Girard, P. M., E. Riballo, A. C. Begg, A. Waugh, and P. A. Jeggo.** 2002. Nbs1 promotes ATM dependent phosphorylation events including those required for G1/S arrest. Oncogene **21:**4191–4199.
17. **Groisman, R., J. Polanowska, I. Kuraoka, J. Sawada, M. Saijo, R. Drapkin, A. F. Kisselev, K. Tanaka, and Y. Nakatani.** 2003. The ubiquitin ligase activity in the DDB2 and CSA complexes is differentially regulated by the COP9 signalosome in response to DNA damage. Cell **113:**357–367.

18. **Hanawalt, P. C., J. M. Ford, and D. R. Lloyd.** 2003. Functional characterization of global genomic DNA repair and its implications for cancer. Mutat. Res. **544:**107–114.
19. **Herskowitz, J., M. A. Jacoby, and S. H. Speck.** 2005. The murine gammaherpesvirus 68 M2 gene is required for efficient reactivation from latently infected B cells. J. Virol. **79:**2261–2273.
20. **Husain, S. M., E. J. Usherwood, H. Dyson, C. Coleclough, M. A. Coppola, D. L. Woodland, M. A. Blackman, J. P. Stewart, and J. T. Sample.** 1999. Murine gammaherpesvirus M2 gene is latency-associated and its protein a target for $CD8^+$ T lymphocytes. Proc. Natl. Acad. Sci. USA **96:**7508–7513.
21. **Jacoby, M. A., H. W. Virgin IV, and S. H. Speck.** 2002. Disruption of the M2 gene of murine gammaherpesvirus 68 alters splenic latency following intranasal, but not intraperitoneal, inoculation. J. Virol. **76:**1790–1801.
22. **Kobayashi, J., A. Antoccia, H. Tauchi, S. Matsuura, and K. Komatsu.** 2004. NBS1 and its functional role in the DNA damage response. DNA Repair (Amsterdam) **3:**855–861.
23. **Lagunoff, M., and P. A. Carroll.** 2003. Inhibition of apoptosis by the gammaherpesviruses. Int. Rev. Immunol. **22:**373–399.
24. **Lau, A., K. M. Swinbank, P. S. Ahmed, D. L. Taylor, S. P. Jackson, G. C. Smith, and M. J. O'Connor.** 2005. Suppression of HIV-1 infection by a small molecule inhibitor of the ATM kinase. Nat. Cell Biol. **7:**493–500.
25. **Lee, J. H., and T. T. Paull.** 2005. ATM activation by DNA double-strand breaks through the Mre11-Rad50-Nbs1 complex. Science **308:**551–554.
26. **Leupin, O., S. Bontron, C. Schaeffer, and M. Strubin.** 2005. Hepatitis B virus X protein stimulates viral genome replication via a DDB1-dependent pathway distinct from that leading to cell death. J. Virol. **79:**4238–4245.
27. **Liang, X., Y. C. Shin, R. E. Means, and J. U. Jung.** 2004. Inhibition of interferon-mediated antiviral activity by murine gammaherpesvirus 68 latency-associated M2 protein. J. Virol. **78:**12416–12427.
28. **Lilley, C. E., C. T. Carson, A. R. Muotri, F. H. Gage, and M. D. Weitzman.** 2005. DNA repair proteins affect the lifecycle of herpes simplex virus 1. Proc. Natl. Acad. Sci. USA **102:**5844–5849.
29. **Lin, G. Y., and R. A. Lamb.** 2000. The paramyxovirus simian virus 5 V protein slows progression of the cell cycle. J. Virol. **74:**9152–9166.
30. **Matsuoka, S., M. Huang, and S. J. Elledge.** 1998. Linkage of ATM to cell cycle regulation by the Chk2 protein kinase. Science **282:**1893–1897.
31. **McGowan, C. H., and P. Russell.** 2004. The DNA damage response: sensing and signaling. Curr. Opin. Cell Biol. **16:**629–633.
32. **McKinnon, P. J.** 2004. ATM and ataxia telangiectasia. EMBO Rep. **5:**772–776.
33. **Paull, T. T., E. P. Rogakou, V. Yamazaki, C. U. Kirchgessner, M. Gellert, and W. M. Bonner.** 2000. A critical role for histone H2AX in recruitment of repair factors to nuclear foci after DNA damage. Curr. Biol. **10:**886–895.
34. **Petrini, J. H., and T. H. Stracker.** 2003. The cellular response to DNA double-strand breaks: defining the sensors and mediators. Trends Cell Biol. **13:**458–462.
35. **Rappold, I., K. Iwabuchi, T. Date, and J. Chen.** 2001. Tumor suppressor p53 binding protein 1 (53BP1) is involved in DNA damage-signaling pathways. J. Cell Biol. **153:**613–620.
36. **Schultz, L. B., N. H. Chehab, A. Malikzay, and T. D. Halazonetis.** 2000. p53 binding protein 1 (53BP1) is an early participant in the cellular response to DNA double-strand breaks. J. Cell Biol. **151:**1381–1390.
37. **Shen, Y. H., B. Utama, J. Wang, M. Raveendran, D. Senthil, W. J. Waldman, J. D. Belcher, G. Vercellotti, D. Martin, B. M. Mitchelle, and X. L. Wang.** 2004. Human cytomegalovirus causes endothelial injury through the ataxia telangiectasia mutant and p53 DNA damage signaling pathways. Circ. Res. **94:**1310–1317.
38. **Shirata, N., A. Kudoh, T. Daikoku, Y. Tatsumi, M. Fujita, T. Kiyono, Y. Sugaya, H. Isomura, K. Ishizaki, and T. Tsurumi.** 2005. Activation of ataxia telangiectasia-mutated DNA damage checkpoint signal transduction elicited by herpes simplex virus infection. J. Biol. Chem. **280:**30336–30341.
39. **Simas, J. P., S. Marques, A. Bridgeman, S. Efstathiou, and H. Adler.** 2004. The M2 gene product of murine gammaherpesvirus 68 is required for efficient colonization of splenic follicles but is not necessary for expansion of latently infected germinal centre B cells. J. Gen. Virol. **85:**2789–2797.
40. **Stracker, T. H., C. T. Carson, and M. D. Weitzman.** 2002. Adenovirus oncoproteins inactivate the Mre11-Rad50-NBS1 DNA repair complex. Nature **418:**348–352.
41. **Strickland, P. T., O. Nikaido, T. Matsunaga, and J. M. Boyle.** 1992. Further characterization of monoclonal antibody indicates specificity for (6-4)-dipyrimidine photoproducts. Photochem. Photobiol. **55:**723–727.
42. **Sunil-Chandra, N. P., J. Arno, J. Fazakerley, and A. A. Nash.** 1994. Lymphoproliferative disease in mice infected with murine gammaherpesvirus 68. Am. J. Pathol. **145:**818–826.
43. **Svejstrup, J. Q.** 2002. Mechanisms of transcription-coupled DNA repair. Nat. Rev. Mol. Cell Biol. **3:**21–29.
44. **Takacs-Vellai, K., T. Vellai, A. Puoti, M. Passannante, C. Wicky, A. Streit, A. L. Kovacs, and F. Muller.** 2005. Inactivation of the autophagy gene bec-1 triggers apoptotic cell death in C. elegans. Curr. Biol. **15:**1513–1517.
45. **Taylor, T. J., and D. M. Knipe.** 2004. Proteomics of herpes simplex virus replication compartments: association of cellular DNA replication, repair, recombination, and chromatin remodeling proteins with ICP8. J. Virol. **78:**5856–5866.
46. **Thiriet, C., and J. J. Hayes.** 2005. Chromatin in need of a fix: phosphorylation of H2AX connects chromatin to DNA repair. Mol. Cell **18:**617–622.
47. **Tornaletti, S.** 2005. Transcription arrest at DNA damage sites. Mutat. Res. **577:**131–145.
48. **Ulane, C. M., and C. M. Horvath.** 2002. Paramyxoviruses SV5 and HPIV2 assemble STAT protein ubiquitin ligase complexes from cellular components. Virology **304:**160–166.
49. **Ulane, C. M., A. Kentsis, C. D. Cruz, J. P. Parisien, K. L. Schneider, and C. M. Horvath.** 2005. Composition and assembly of STAT-targeting ubiquitin ligase complexes: paramyxovirus V protein carboxyl terminus is an oligomerization domain. J. Virol. **79:**10180–10189.
50. **Unal, E., A. Arbel-Eden, U. Sattler, R. Shroff, M. Lichten, J. E. Haber, and D. Koshland.** 2004. DNA damage response pathway uses histone modification to assemble a double-strand break-specific cohesin domain. Mol. Cell **16:**991–1002.
51. **van Attikum, H., O. Fritsch, B. Hohn, and S. M. Gasser.** 2004. Recruitment of the INO80 complex by H2A phosphorylation links ATP-dependent chromatin remodeling with DNA double-strand break repair. Cell **119:**777–788.
52. **Vidanes, G. M., C. Y. Bonilla, and D. P. Toczyski.** 2005. Complicated tails: histone modifications and the DNA damage response. Cell **121:**973–976.
53. **Virgin, H. W., IV, P. Latreille, P. Wamsley, K. Hallsworth, K. E. Weck, A. J. Dal Canto, and S. H. Speck.** 1997. Complete sequence and genomic analysis of murine gammaherpesvirus 68. J. Virol. **71:**5894–5904.
54. **Ward, I. M., K. Minn, K. G. Jorda, and J. Chen.** 2003. Accumulation of checkpoint protein 53BP1 at DNA breaks involves its binding to phosphorylated histone H2AX. J. Biol. Chem. **278:**19579–19582.
55. **Westphal, C. H.** 1997. Cell-cycle signaling: Atm displays its many talents. Curr. Biol. **7:**R789–R792.
56. **Wilkinson, D. E., and S. K. Weller.** 2004. Recruitment of cellular recombination and repair proteins to sites of herpes simplex virus type 1 DNA replication is dependent on the composition of viral proteins within prereplicative sites and correlates with the induction of the DNA damage response. J. Virol. **78:**4783–4796.
57. **Wittschieben, B. B., and R. D. Wood.** 2003. DDB complexities. DNA Repair (Amsterdam) **2:**1065–1069.
58. **You, Z., C. Chahwan, J. Bailis, T. Hunter, and P. Russell.** 2005. ATM activation and its recruitment to damaged DNA require binding to the C terminus of Nbs1. Mol. Cell. Biol. **25:**5363–5379.
59. **Young, L. S., and A. B. Rickinson.** 2004. Epstein-Barr virus: 40 years on. Nat. Rev. Cancer **4:**757–768.
60. **Zimmerman, E. S., J. Chen, J. L. Andersen, O. Ardon, J. L. DeHart, J. Blackett, S. K. Choudhary, D. Camerini, P. Nghiem, and V. Planelles.** 2004. Human immunodeficiency virus type 1 Vpr-mediated G_2 arrest requires Rad17 and Hus1 and induces nuclear BRCA1 and γ-H2AX focus formation. Mol. Cell. Biol. **24:**9286–9294.